Theor Appl Climatol (2015) 120:55–67
DOI 10.1007/s00704-014-1150-y

ORIGINAL PAPER

The impact of basic state on quasi-biennial periodicity of central Pacific ENSO over the past decade

Ruihuang Xie · Fei Huang · Fei-Fei Jin · Jian Huang

Received: 22 September 2013 / Accepted: 29 March 2014 / Published online: 22 April 2014

Abstract El Niño/Southern Oscillation (ENSO) phenomenon lately appears to have a much fast pace with four warming events in the past decade (2002–2012). Three out of four events have their warming centers confined in the equatorial central Pacific. It is argued that the anomalous zonal sea currents are responsible for the fast transition of the central Pacific warming. Furthermore, based on the heat budget analysis, it is found that zonal advective feedback appears to play an important role in the phase transition of central Pacific ENSO, although the thermocline feedback process that is essential for ENSO, as delineated by the recharge/discharge oscillator theory, also contributes but mainly in the eastern Pacific. A stability analysis is performed using a simple stripped-down coupled model with two different basic state settings derived from the periods over 1982–2001 and 2002–2012, respectively. In the two periods, the basic states show different distribution along the equator and the leading ENSO-like eigen-modes have very different periods and patterns. The mode under the basic state in the earlier period resembles the eastern Pacific ENSO with a period about 5 years, whereas under the basic state in the recent decade, the ENSO mode becomes more like the observed central Pacific ENSO with a period about 2 years. The slow eastern Pacific ENSO mode is dominated by the thermocline feedback and behaves more like the recharge oscillator, whereas the zonal advective feedback plays a significant role in the fast-paced central Pacific ENSO mode. These results are roughly consistent with the broad features of two types of ENSO. In addition, the zonal advective feedback contributes to the phase transitions of both types of ENSO-like modes. In a word, the recent fast-paced ENSO activities in the central Pacific is suggested due to the dominance of zonal advective feedback favored by the tropical Pacific basic state conditions in the past decade.

R. Xie · F. Huang (✉)
Department of Marine Meteorology, Physical Oceanography Laboratory and Key Laboratory of Ocean–Atmosphere Interaction and Climate in Universities of Shandong, Ocean University of China, Qingdao, Shandong 266100, China
e-mail: huangf@ouc.edu.cn

R. Xie
Key Laboratory of Ocean Circulation and Waves, Institute of Oceanology, Chinese Academy of Sciences, Qingdao 266071, China

F.-F. Jin
Department of Meteorology, School of Ocean and Earth Sciences and Technology, University of Hawaii at Manoa, Honolulu, HI 96822, USA

J. Huang
Guangzhou Institute of Tropical and Marine Meteorology, China Meteorological Administration, Guangzhou, Guangdong 510080, China

1 Introduction

The conventional El Niño-Southern Oscillation (ENSO) is characterized by anomalous sea surface temperature (SST) broadly extending from the South American coast to the date line (Rasmusson and Carpenter 1982). In the recent decade, a different type of El Niño/ENSO has been detected with the warming center confined in the central Pacific. Various names has been given to describe this new El Niño/ENSO type by different researchers, e.g., date line El Niño (Larkin and Harrison 2005), El Niño Modoki (Ashok et al. 2007), central Pacific ENSO (Kao and Yu 2009), and cold tongue El Niño (Kug et al. 2009). We adopted the terminology of central Pacific (CP) and eastern Pacific (EP) El Niño in this study due to the apparently different SST anomaly centers. The CP El Niño is found to have different impacts on the global climate compared with the conventional one (Weng et al. 2007; Yeh et al. 2009; Zhang et al. 2011). For instance, more precipitation is found over the central and western Pacific

other than the central and eastern Pacific during CP El Niño (Ashok et al. 2007; Kug et al. 2009). As a result, the anomalous atmospheric heating causes a different wave-train to influence the western North Pacific (Zhang et al. 2011) and mid-latitude (Yeh et al. 2009). Interestingly, CP El Niño exhibits a tendency of roughly quasi-biennial occurrence in the recent decade, and matches the long-suggested period of about 2 years (Trenberth 1976, 1984; Barnett 1991; Wang and An 2005), in addition to the major period of 4 years. However, the debates about the periodicity of CP ENSO are still undergoing. For instance, Weng et al. (2007) and Ren et al. (2013) argued that CP ENSO showed large decadal variability besides the quasi-biennial variation. On the other hand, Kao and Yu (2009) found significant 2-year variability but weak decadal/interdecadal in their CP ENSO index. In order to avoid confusion, this paper only emphasizes on its quasi-biennial periodicity. So far, the different warming pattern, major period and climate impact of CP El Niño, compared with those of EP El Niño, further enrich the diversity and prosperous spectrum of the phenomena of ENSO that are long discussed in the early ENSO studies (Suarez and Schopf 1988; Battisti and Hirst 1989; Jin 1997a; b; Fedorov and Philander 2000, 2001, hereafter FP01; Bejarano and Jin 2008, hereafter BJ08).

The abovementioned changes of ENSO are accompanied by the shift of basic state in the tropical Pacific around late 1990s (Xiang et al. 2013; Hu et al. 2013), which is featured by strengthened trade winds, enhanced low-level atmospheric divergence and shoaled thermocline in the eastern Pacific after 2000. Therefore, it is more difficult for the initial unstable air–sea interaction to propagate eastward because of the enhanced divergence. Consequently, a central Pacific SST warming event develops locally. McPhaden (2012) pointed out that the shift towards more CP versus EP El Niños in the past decade was linked with decreased impact of thermocline feedback on ENSO SST development, and this shift was also accompanied with decreased warm water volume (WWV, Meinen and McPhaden 2000) variations and reduced leading time of WWV to ENSO SST anomalies. Such a decreasing was also confirmed by the recent work of Kumar and Hu (2013). Although this mechanism can help understand the pattern change of ENSO, it is inadequate to interpret the shift of the periodicity around late 1990s, which is related to the relative importance of two major feedbacks that have different timescales (FP01). Different types of basic state are favorable for the dominance of different feedbacks (FP01; BJ08).

By far, both the theoretical and modeling studies have revealed that the thermocline feedback (vertical advection of anomalous subsurface temperature by mean upwelling) is essential to interpret the slow physics (~4 years) of the coupled dynamics of ENSO (Jin 1996, 1997a, b; Burgers et al. 2005), and this feedback is favored by a deep thermocline condition (FP01; BJ08). In addition, *the zonal advective feedback*, which is interpreted as anomalous zonal advection of mean temperature gradient by anomalous zonal current, can support the fast component of ENSO. For instance, it is the key element of the advective–reflective ENSO oscillator (Picaut et al. 1997), which interpreted the ENSO phenomenon as a forward-backward motion of the warm pool edge driven by the oceanic Rossby and Kelvin waves. Besides, FP01 emphasized the role of this feedback in the formation of a local ENSO mode with a short period, while BJ08, using a similar approach as FP01, further inferred that the life cycle of the quasi-biennial ENSO resembles an advective–reflective oscillator. Both FP01 and BJ08 suggested that this feedback plays a crucial role in producing ENSO when the thermocline depth in the eastern Pacific is relatively shallow and trade winds are relatively strong. Based on the observation analysis, Kug et al. (2009) concluded that zonal advection feedback plays a key role in the developing phase of the warm pool (CP) type of El Niño, while the thermocline feedback contributes less. In the tropical Pacific, it is the combination of these two feedbacks in various percentages that gives ENSO prosperous spectrum (An et al. 1999; Jin and An 1999; An and Jin 2001; FP01; BJ08). Thus far, both the theoretical and observational researches have provided strong supports and perspectives to the fast-paced ENSO over the past decade when the tropical Pacific is undergoing stronger trades and shallower thermocline in the eastern Pacific. Motivated by FP01 and BJ08, we first connect the observational evidence of CP El Niño to their theoretical studies, then a pair of experiments are designed in a simple ENSO model to investigate the sensitiveness of ENSO modes to the mean states, as done by Kang et al. (2004). A comparison will be applied to highlight the relative importance of the aforementioned two feedbacks under different mean states. This is helpful for better understanding the quasi-biennial occurrence of ENSO in the central Pacific.

This paper will be organized as follows: The data and methodology are introduced in Section 2. Section 3 investigates the major characteristics of the ENSO in the central Pacific. In Section 4, two sets of stability analyses are performed using Jin's recharge model to obtain and compare the leading modes under two different basic states of the tropical Pacific. Section 5 gives summary and conclusions.

2 Data and methodology

The datasets used here are the monthly mean of sea surface temperature from HadISST (Rayner et al. 2003), wind stress, ocean current, and ocean subsurface temperature from NCEP Global Ocean Data Assimilation System (GODAS) (Ji et al. 1995; Behringer et al. 1998). All the variables are preprocessed by removing their variabilities that are shorter than 3 months. Anomalous quantities are obtained by removing the

climatological monthly mean of the period 1981–2010. For a comparison, satellite observations of sea current from OSCAR (Bonjean and Lagerloef 2002) and sea level from AVISO TOPEX/ERS/Jason1 merged altimeter datasets[1] are employed to for diagnostic analysis. The basic mean for these two variables are the monthly mean of 1993–2010 for the maximum coverage. In order to focus on the quasi-biennial band, band-pass filter of 18 to 36 months is applied to extract the 2-year component.

The simple ENSO model adopted in this study is the recharge/discharge ENSO model (Jin 1997b). This model is a stripped-down (two strips) wind-driven shallow water ocean model under long-wave approximation on the β-plane. It describes the thermocline dynamics associated with the Kelvin waves at the equatorial strip and Rossby waves at the off-equatorial strip, and the two strips are dynamically connected by Sverdrup transport induced by interior ocean current across the basin. Then the changes of the equatorial thermocline determine SST anomalies (SSTA), which in turn affect the wind stress anomalies to generate oceanic waves. The detailed description of this model will be shown in Section 4.

3 Observed features of ENSO in the central pacific

Traditional Niño 3 and Niño 4 indices averaged in 10 El Niño winters (November to February season) during 1982–2012 are shown in Fig. 1. During these ten winters, there are six (four) winters when Niño 3 index (SST anomalies averaged over the region 5° S–5° N, 150° W–90° W) exceeds (drops below) the Niño 4 index (SST anomalies averaged over the region 5° S–5° N, 160° E–150° W), indicating that EP El Niño (CP El Niño) events occurred in these winters. Moreover, five of six EP El Niño events (three of four CP El Niño events) occurred before (after) the beginning of this century. As pointed out by Kug et al. (2009), the major SST anomalies of La Niña events has moved westward to Niño 3.4 region (5° S–5° N, 170° W–120° W), so the ten La Niña events are measured by the Niño 3.4 index without being classified into two types. Therefore, the tendency of increasing occurrence of CP versus EP El Niño is evident during the last decade. This trend is robust even using other complex Niño indices, such as those summarized by Ren and Jin (2011). For clear comparison, the early 20 years (1982–2001) which is dominated by EP El Niño variability is names as the early period, while the last 11 years (2002–2012) is called the late period. In the next text, this period is also expressed as the last, past or recent decade.

The major characteristics of the El Niño or ENSO events in the early period are extensively investigated in some previous researches mentioned in Section 1, and will not be repeated here. The keynote will be the features of the El Niño or ENSO events and their mechanism exploration in the late period, when the tropical Pacific experiences a La Niña-like mean state change (Xiang et al. 2013; Hu et al. 2013). In order to focus on the quasi-biennial variation of the SST anomalies, we first take a look at the equatorial cooperated atmospheric and oceanic variables during the late period. Figure 2 shows the equatorial anomalous SST, zonal wind stress, zonal sea current, and thermocline depth (defined by the depth of 20 °C isotherm) averaged between 5° S to 5° N. The SSTA roughly shows five cycles with fairly regular oscillation in 11 years. The oceanic and atmospheric variables oscillate resonantly and show the features of ENSO, e.g., the slightly westward propagating of SSTA and zonal sea current flowing from the central Pacific to western Pacific during their decaying stages. The 2009/2010 event is the only one without above features. However, it is not clear in this figure if the western propagation of the anomalous sea current plays any role in the phase transition of the central Pacific ENSO. Note that the out-of-phase zonal wind stress distribution along the equator and the anomalous westerly are confined to the west of 160° W, reflecting the fact that the central Pacific ENSO develops locally other than basin-wide (Kao and Yu 2009; Kug et al. 2009; Xie et al. 2013). The evolution of the anomalous air–sea coupling has been summarized by Hu et al. (2012), who suggested that stronger (weaker) and more eastward extended (westward confined) westerly wind along the equatorial Pacific in early months of a year is associated with active (suppressed) air–sea interaction over the cold tongue/the Intertropical Convergence Zone complex, as well as more (less) intensive oceanic thermocline feedback, favoring the EP (CP) El Nino development. In the eastern equatorial Pacific, the anomalous easterlies are weak but the anomalies in the sea current are strong, which means that the local Ekman balance is not valid on the equator, therefore the large current anomalies have to be associated with the reflection of the off-equatorial oceanic Rossby waves (Kang et al. 2004; Kug et al. 2009). The anomalous westerly over the central-western Pacific excites westward-propagating upwelling Rossby waves off the equator, then the Rossby waves reflect at the western boundary as eastward-propagating upwelling Kelvin waves and alter the equatorial current.

Such a westward-propagating SSTA is similar to the analytical solution in Neelin and Jin (1993), which shows strong sea current anomalies in the central Pacific. A fast, near-annual "Pacific Ocean Basin" mode is exhibited by the solution (Jin et al. 2003; Kang et al. 2004). In FP01 and BJ08, they obtain numerical model solutions with a dominant period of 2 years and westward phase propagation under the mean states of strong trades and shallow thermocline. They conclude that the SST variations of these solutions depend mainly on the anomalous advection of the mean zonal temperature gradient by the

[1] The altimeter products were produced by the CLS Space Oceanography Division as part of the Environment and Climate EU ENACT project (EVK2-CT2001-00117) and with support from CNES.

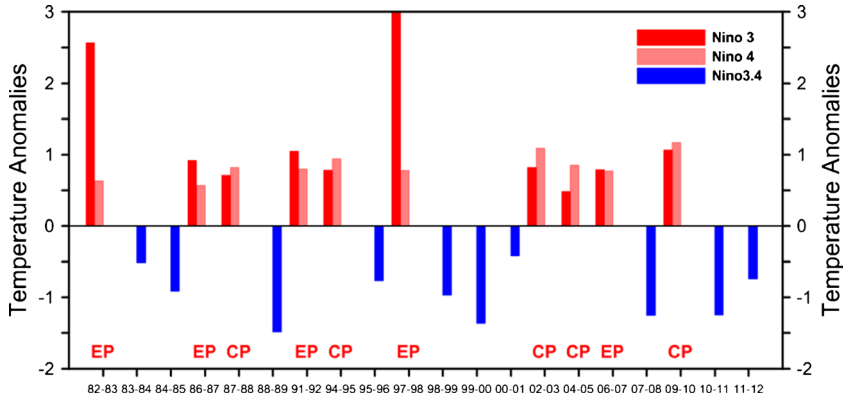

Fig. 1 Niño 3 (*dark red*) and Niño 4 (*light red*) SST anomalies for El Niño and Niño 3.4 (*blue*) SST anomalies for La Niña events between 1982 and 2012. Values are for the mature November to February season. Eastern Pacific (EP) and central Pacific (CP) El Niño events are *labeled on the bottom*. The classification of these two types is described in the text

anomalous zonal sea current (*the zonal advective feedback*). The Pacific mean state in the late period resembles the model design of FP01 and BJ08, and the observed periodicity and phase propagation fit the numerical analysis. These results demonstrate the role of anomalous zonal sea current in the life cycle of ENSO in the central Pacific.

The spatial evolving patterns are further examined using composite of SST, wind stress, thermocline depth and sea currents anomalies in five phases (shown in Fig. 3). The lag 0 phase means the mature phase of ENSO, which is chosen as December of year 2002, 2004, 2006, 2009, while the lag −6, −3 and 3, 6 months indicate the onset, developing, and transition, decaying phases, respectively. In the onset phase (lag −6), the westerly anomalies are detected in the western north Pacific before the equatorial SST anomalies are established (Fig. 3a). Some early studies reported that these wind anomalies may be induced by forcing from the North Pacific via the Seasonal Footprinting Mechanism (Vimont et al. 2001, 2003, 2009; Yu and Kim 2011). The anomalous westerlies are enhanced 3 months later, as well as the SST anomalies (Fig. 3b).

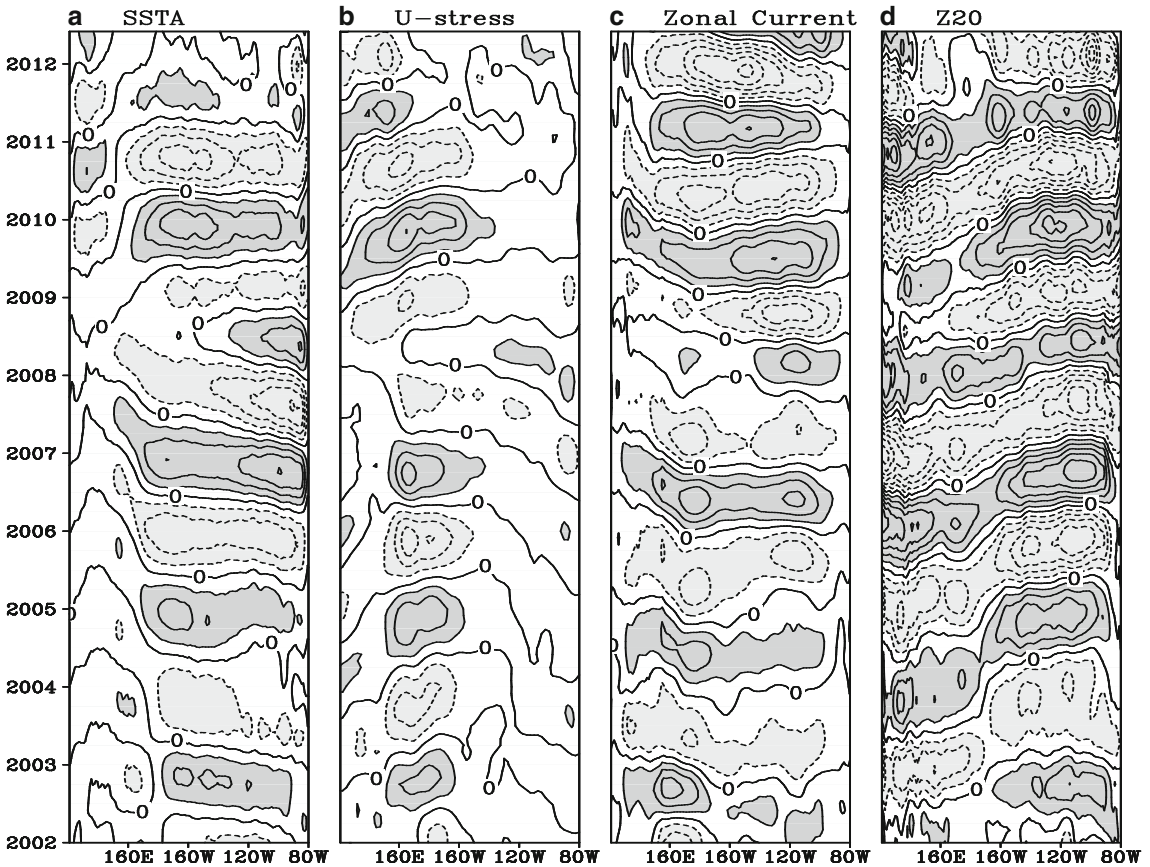

Fig. 2 Longitude–time cross-section of the equatorial averaged (5° S–5° N) SST (**a**), zonal wind stress (**b**), zonal sea current (**c**, upper 50 m mean) and thermocline depth (**d**, the depth of 20 °C isotherm) anomalies for the period of Jan 2002 to Jun 2012. The intervals for **a** to **d** are 0.3 °C, 0.05 Pa, 5 cm/s, and 2.5 m, respectively. All variables are filtered by an 18–36 months band-pass filterer

During the mature phase, the SST anomalies pattern shows a warming center located in the equatorial central Pacific (Fig. 3c), and the anomalous eastward wind stress extends to the central Pacific while weak westward wind stress anomalies occur over the eastern Pacific. At the transition phase (Fig. 3d), the coupled SST and wind stress anomalies both decrease. Three months later, the positive SSTA vanishes and negative SSTA starts to develop in the eastern Pacific (Fig. 3e). This wind-SST evolving pattern is, to some extent, consistent with the typical description of ENSO by Rasmusson and Carpenter (1982).

The evolving patterns of the thermocline depth and sea current anomalies show features of basin-wide recharge/discharge of the ocean heat content, although the air–sea interaction on the sea surface appears as local process. At the onset phase (lag −6), excited by anomalous westerlies in the western Pacific, anomalous eastward sea current appears in the equatorial Pacific (Fig. 3f), which drives the warmer water to the central-eastern Pacific. Subsequently, a band of weak positive thermocline depth anomalies appears in the equatorial central-eastern Pacific and anomalous heat content is recharged in that region. In the following several months, the recharging process continues as the eastward equatorial sea current anomalies are gradually enhanced by the wind stress. The thermocline depth anomalies in the central-eastern Pacific reach the maximum in the peak phase (Fig. 3h). However, at the same time, a band of anomalous weak westward currents appear to the west of the thermocline depth maximum center. These currents can lead to the shoaling of the thermocline depth. According to Kug et al. (2009), these anomalous westward sea currents are related to two components. One is the pressure gradient forced westward current, the other is the reflected upwelling Kelvin wave from the western boundary. At the transition phase, the westward sea current anomalies are further intensified (Fig. 3i). As a result, the equatorial thermocline depth anomalies gradually turn to negative. However, the off-equatorial thermocline depth anomalies in turn become positive, which means the equatorial heat content starts to discharge. Finally, at the decaying phase (Fig. 3j), anomalous strong westward sea currents appear over the basin-wide equatorial Pacific and the thermocline depth anomalies are negative along the equatorial Pacific, while the off-equatorial thermocline depth anomalies become significantly positive. The evolution of the satellite observed surface sea current and sea level height anomalies are similar to those from GODAS reanalysis, except for the location of the reversal of equatorial sea current anomalies during the peak phase (Fig. 3m). The reversed westward sea current anomalies appear in the central and eastern equatorial Pacific other than in central equatorial Pacific as the GODAS data shows (Fig. 3h). It still supports the wave reflection mechanism, because the eastward sea current anomalies are weaker than those in Fig. 3l. Considering the mismatch of intensities of wind stress and sea current anomalies, the

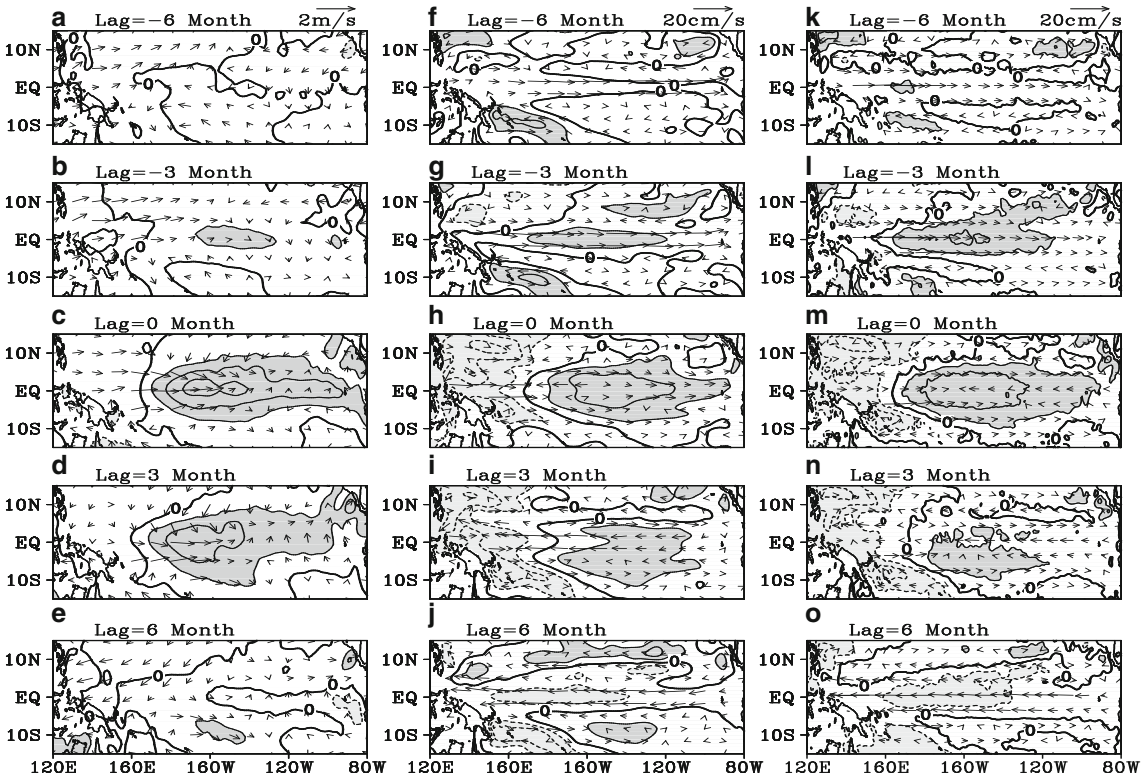

Fig. 3 Composite of SST and wind stress anomalies (**a**–**e**), thermocline depth and sea currents anomalies (**f**–**j**). The intervals for SST and thermocline depth anomalies are 0.3 °C and 2.5 m, respectively. Figures **k**–**o** are similar to **f**–**j**, but for satellite observed surface current (vector) and sea level height (contour, interval: 2 cm) anomalies. All variables are filtered by an 18–36 months band-pass filterer

westward sea current anomalies associated with the reflected Kelvin waves are the only plausible factors to counteract the wind-induced eastward sea current anomalies. Overall, the evolution of the thermocline depth displays a clear recharge/discharge process (positive/negative tendency of equatorial thermocline depth) between the equatorial and off-equatorial regions. During this process, the anomalous zonal current plays a noticeable role in the phase transition of the ENSO.

The dynamical diagnosis above provides a qualitative view to distinguish the role of the anomalous zonal sea currents and thermocline in the ENSO cycle. Nevertheless, we still need quantitative measurements to illustrate the relative importance of these two variables in determining the SST anomalies. Here, a brief heat budget analysis of the mix layer temperature is performed using the following SST equation, as adopted by Kang et al. (2004).

$$\frac{\partial T}{\partial t} \approx \left(-u\frac{\partial \overline{T}}{\partial x} - w\frac{\partial \overline{T}}{\partial z} + w\frac{T_{\mathrm{sub}}}{H_1} \right) + R, \tag{1}$$

where the variables with an overbar indicate monthly climatology, and those without overbar denote monthly mean anomaly. T_{sub} is the depth-averaged temperature anomalies from 50 to 100 m, and H_1 indicates the bottom of the mix layer (50 m). The first, second, and third term at the right side of Eq. 1 describe the zonal advective feedback, the anomalous downwelling advection and the thermocline feedback, respectively. These three terms serve as positive contribution to the growth of ENSO (Jin et al. 2006). All other terms are included in the R term, because they mainly provide a damping effect to SST (Kang et al. 2001; FP01; Kug et al. 2009; Ren and Jin 2013). The SSTA and its tendency along with these three terms are displayed in Fig. 4a–e. The figures clearly show that the SST variation in the central Pacific is dominated by the zonal advective feedback, while the other two terms only show significant distributions in the eastern Pacific. It is noticed that the zonal advective feedback leads the SSTA by 1/4 cycle, and it provides the negative force for the SST anomalies to decay and turn to the negative phase. This result is different from the ENSO variation before 2002, when the ENSO-related SST anomalies are mainly controlled by the thermocline feedback (An et al. 1999; Jin and An 1999; Kang et al. 2001).

4 Unstable quasi-biennial mode in a recharge/discharge model

The previous section shows the observation evidences for the quasi-biennial ENSO oscillation in the last decade. In this section, we will employ Jin's recharge/discharge model (Jin 1997b; An and Jin 2001) to examine the QB oscillation with the observed basic state in the past decade and to compare the results with those in the previous studies.

4.1 The recharge/discharge model

The model is derived from the oceanic component of the Zebiak-Cane (ZC) model (Zebiak and Cane 1987). The simplification and non-dimensionalization can be seen in Jin (1997b). The final controlling equations of equatorial thermocline (h_{e}) and off-equatorial thermocline (h_{n}) are given below.

$$(\partial_{\mathrm{t}} + \varepsilon_{\mathrm{m}})(h_{\mathrm{e}} - h_{\mathrm{n}}) + \partial_{\mathrm{x}} h_{\mathrm{e}} = \tau_{\mathrm{xe}}, \tag{2}$$

$$(\partial_{\mathrm{t}} + \varepsilon_{\mathrm{m}})h_{\mathrm{n}} - \partial_{\mathrm{x}} h_{\mathrm{n}}/y_{\mathrm{n}}^2 = \partial_{\mathrm{y}}(\tau_{\mathrm{x}}/y)\big|_{y=y_{\mathrm{n}}} = -\theta/y_{\mathrm{n}}^2 \cdot \tau_{\mathrm{xe}}. \tag{3}$$

Here ε_{m} means dynamical damping rate, and is taken as $(2.5\ \mathrm{years})^{-1}$, θ is about 1.0–1.25, τ_{xe} is the zonal wind stress anomaly evaluated in the equatorial strip, and y_{n} is equal to 2, which means 5–6° off equator. The Eq. 2 describes the Kelvin waves along the equator with an inclusion of the projection of Rossby waves (indicated by h_{n}), and Eq. 3 retains all the long Rossby waves. For simplification of dynamics, hemispheric symmetry of system is assumed, and the boundary conditions are assumed as no normal motion at the eastern boundary and zero integrated mass flux at the western boundary (Cane and Sarachik 1981; Jin 1997b). So the western and eastern boundary conditions for the two-strip model can be re-written as

$$h_{\mathrm{n}}(x_{\mathrm{E}}) = r_{\mathrm{E}} \times h_{\mathrm{e}}(x_{\mathrm{E}}), \quad h_{\mathrm{e}}(x_{\mathrm{W}}) = r_{\mathrm{W}} \times h_{\mathrm{n}}(x_{\mathrm{W}}), \tag{4}$$

where x_{E} and x_{W} indicate eastern and western boundaries, r_{E} and r_{W} are reflection parameters at the boundaries, and they are set to 0.9 and 0.75, respectively, implying incomplete wave reflection and energy leaking at both boundaries. The choices of these two parameters are according to Jin (1997b), who examined the relevance of the model parameters to the contribution of boundary currents in the recharge/discharge of the equatorial heat content.

A change of SST can be expressed by the thermodynamics of a constant depth of mixed layer embedded in the upper layer ocean. Only the dominant processes are considered, and the equatorial SST anomalies equation is written as:

$$\partial_{\mathrm{t}} T_{\mathrm{e}} = -c(x)T_{\mathrm{e}} + \gamma(x)h_{\mathrm{e}} + a(x)u_{\mathrm{m}}, \tag{5}$$

where.

$$c(x) = \frac{L}{c_0}\left(\varepsilon_{\mathrm{T}} + \frac{\overline{w_1}}{H_{1.5}}\right), \quad \gamma(x) = \frac{H}{\Delta T}\frac{L}{c_0}\frac{\partial T_{\mathrm{sub}}}{\partial z}\frac{\overline{w_1}}{H_{1.5}}, \quad a(x) = -\frac{L}{\Delta T}\frac{\partial \overline{T_{(x)}}}{\partial x}, \tag{6}$$

The equatorial SST anomalies T_{e} are non-dimensionalized by ΔT of 7.5 °C, u_{m} is the zonal sea current along the equator and mathematically it is equal to $h_{\mathrm{e}} - h_{\mathrm{n}}$ in this model. L is the width of the Pacific basin, and c_0 is the internal gravity wave speed. The first term at the right side represents the oceanic damping term which consists of a Newtonian cooling with the damping

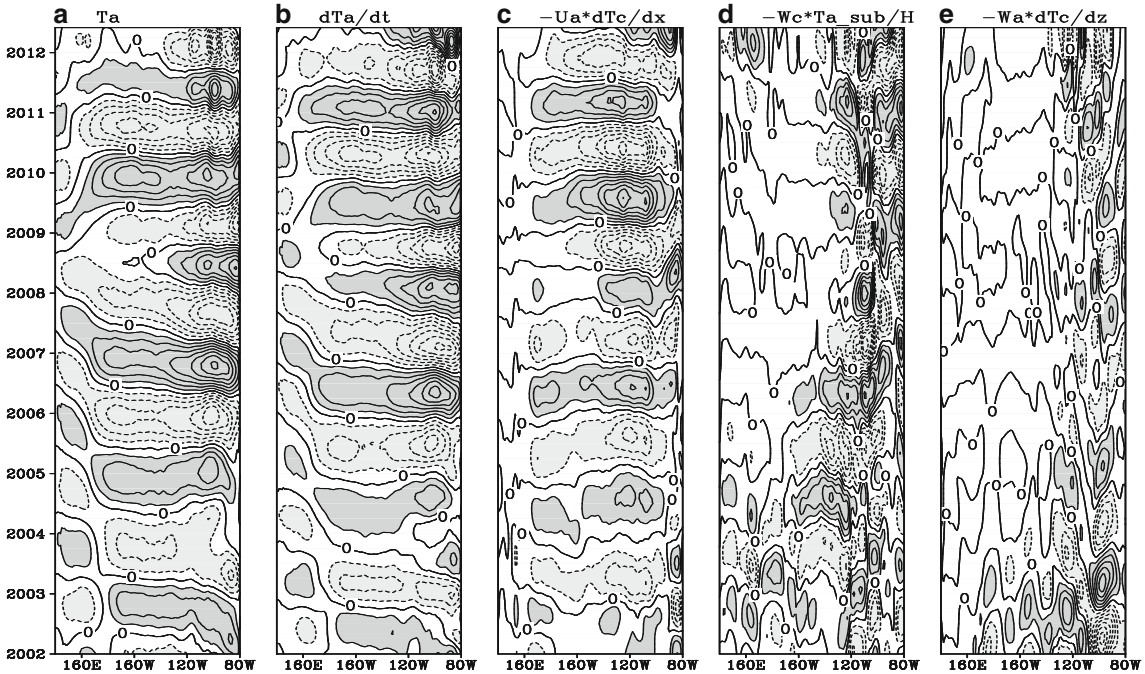

Fig. 4 Longitude–time cross-section of SST anomalies (**a**), SST tendency (**b**), anomalous zonal advective feedback term (**c**), anomalous thermocline displacement term (**d**) and anomalous upwelling of mean vertical temperature term (**e**). The intervals are 0.3 °C for (**a**) and 2.5×10^{-8} °C/s for (**b**–**e**). All terms are filtered by an 18–36 months band-pass filter

rate of $(125\ \text{days})^{-1}$ and the vertical advection of the equatorial SST anomalies by mean upwelling $\overline{w_1}$ at the depth $H_{1.5}$ (50 m). It must be noted that, as the coefficient $c(x)$ is positive along the equator (Fig. 5a), the oceanic damping always serves as a restoring force to the SST anomalies, and its contribution to SST tendency will not be specified in the next content. The second term is the tendency term of vertical displacement of thermocline, which is associated with the thermocline feedback (TH hereafter). The third term is the zonal advective feedback (ZA hereafter). Unlike Jin's original recharge model, the SST variation in this model is jointly controlled by the two competing TH and ZA terms. As concluded in FP01, TH (ZA) can support a slow (fast) ENSO mode with eastward (westward) propagating SSTA. When containing only the thermocline feedback and the necessary cooling, Jin's original recharge model supports the ENSO variation of about 4 years (Jin 1997b). Therefore, by adding the ZA term, the model is expected to capture the fast oscillation of ENSO.

The parameters of Eq. 6 are evaluated by the mean states in the periods of 1982–2001 and 2002–2012 from the NCEP GODAS data. Figure 5 shows the longitudinal distributions of the coefficients $c(x)$, $\gamma(x)$, and $a(x)$ along the equator (2° S–2° N averaged) for the early and late periods. As seen in Fig. 5a, compared to the early period, the damping rate in the late period does not show a uniform increasing pattern along the equator. It is enhanced between 170° W and 110° W but weakened around dateline and in the far eastern Pacific. On the other hand, the thermocline feedback coefficients $\gamma(x)$ along the eastern Pacific (east of 160° W) are weaker in the late period (Fig. 5b), indicating weaker impact of thermocline movement on the SST. Moreover, the values of $\gamma(x)$ near the dateline drop below

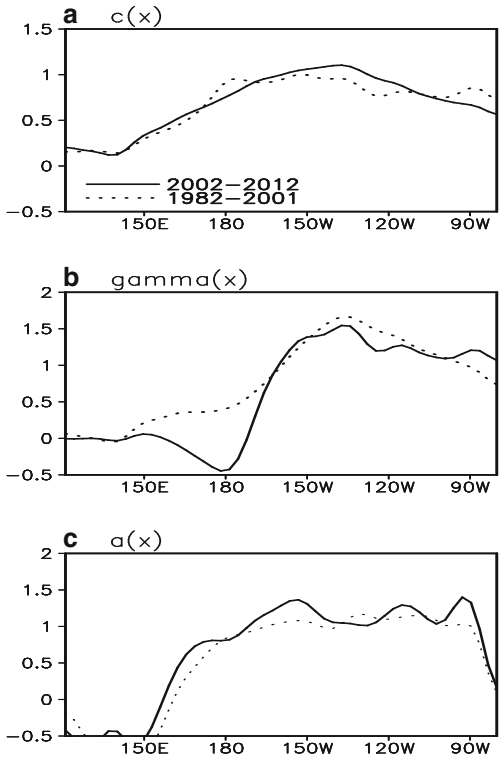

Fig. 5 Longitudinal distribution of the parameters $c(x)$, $\gamma(x)$ and $a(x)$ in the SST equation of Eq. 4. The *solid line* is for the mean state of 2002–2012, and the *dashed line* for 1982–2001

zero in the late period, which results from the negative regression coefficient of subsurface temperature onto thermocline depth when computing $\frac{\partial T_{\mathrm{sub}}}{\partial z}$. The negative values are also found by Thual et al. (2011), although they introduce a different empirical function connecting the thermocline depth and subsurface temperature. The zonal advection coefficients for the late period are stronger than those for the early period (Fig. 5c), which matches the fact that the zonal temperature gradient is enhanced (Xiang et al. 2013).

4.2 Wind stress

In the original version of Jin's model (1997b), the wind stress only responds to the SST anomalies in the eastern Pacific, and it only occurs over the central 1/3 part of the Pacific basin. Despite the primary consideration of simplification in the conceptual research, the limitations of such a description of wind stress are twofold. First, it ignores the wind component that is excited by the local SST anomalies. Second, it mistakes in describing the longitudinal scale of the wind stress. There are evidences from the intermediate models that the structure of the surface wind stress have impact on the oceanic adjustment time scale and the ENSO behavior (Cane et al. 1990; Kirtman 1997; An and Wang 2000). In order to avoid this defect, we adopt a more realistic description of the equatorial zonal wind stress, which is related to equatorial SST anomalies T_{e} through a simplified Gill-type atmosphere model. This wind stress equation is solved by Jin and Neelin (1993) and improved in FP01. It is expressed as:

$$\tau_{\mathrm{xe}} = \mu\lambda A \times \left[\frac{3}{2}\exp\left(\frac{3\varepsilon_a x}{L}\right)\int_{x_W}^{x} T_e \ \exp\left(-\frac{3\varepsilon_a x}{L}\right)\frac{dx}{L} - \frac{1}{2} \ \exp\left(-\frac{\varepsilon_a x}{L}\right)\int_{x}^{x_E} T_{\mathrm{e}} \ \exp\left(\frac{\varepsilon_a x}{L}\right)\frac{dx}{L}\right]. \tag{7}$$

Here μ is the non-dimensionalized air–sea coupling coefficient, and λ is a spatial factor to reduce east winds associated with Kelvin wave near the eastern boundary. It is expressed as $\lambda(x) = 0.5 \times \left\{\tanh\left[\frac{10(x-x_{\mathrm{E}})}{L}\right] + 1\right\}$. The factor A is the dimensional amplitude of wind stress and ε_a is the inverse atmospheric damping. It contains the atmospheric response to both remote and local SST anomalies forcing, as well as wind stress related to both Rossby wave (the first half) and Kelvin wave (the second half). The detailed explanations can be found in Jin and Neelin (1993) and FP01.

With the given values for λ, A, ε_a and other parameters in Table 1, the shape of the wind stress is fixed with its amplitude being determined by the air–sea coupling μ. To determine this parameter, the observed SST anomaly is used to drive the wind stress using increasing μ from 0 to 1.0 with an increment of 0.01. When μ is around 0.4, the simulated and observed wind stress anomaly show comparable amplitudes and standard deviations (Fig. 6), with a pattern correlation of 0.53. The wind stress anomalies during the four major El Niño and La Niña events are simulated successfully with comparable amplitudes (Fig. 6a, b). However, the wind stress anomalies in the eastern Pacific are overestimated due to the systemic defect of the Gill-type atmosphere response (Zebiak 1986), even though the spatial factor λ is adopted here. Along the equator, the simulated wind stress anomalies in the central and western Pacific show high correlation with the observation (Fig. 6c), but the zonal scale of its activity (reflected by the standard deviation) is narrower than the observation (Fig. 6d). Also, errors of the wind stress simulation is reflected by the unreasonable variation over the region east of 160° W, where there is less significant correlation but unreasonably larger variation. Apparently, the description of wind stress captures the variability over the central Pacific, where in the observation the air–sea interaction reaches its maximum. Since the whole recharge model is simplified from the ZC-type model, we expect the coupled process would "forgive" the minor errors in the expression of the wind stress, as Zebiak and Cane (1987) inferred.

Table 1 List of parameters used in the recharge model

Variable	Value	Variable	Value
θ	1.0	ε_{T}	(125 days) $^{-1}$
ε_{m}	(2.5 years)$^{-1}$	$H_{1.5}$	50 m
y_{n}	2.0	x_{W}	120° E
r_{E}	0.9	x_{E}	80° W
r_{W}	0.75	H	150 m
L	15,000 km	ΔT	7.5 °C
c_0	2.9 m/s	A	0.05 Pa/K
ε_{a}	2.5		

4.3 Stability analysis of the recharge model

With this coupling strength (μ=0.41), the eigen-modes of system (2), (3), and (4) through the stability analysis are obtained in a 50-grid system using the mean state of 2002–2012. The performance of the stability analysis is the same as done by Jin (1997b). Only one unstable mode is detected, and it has an e-folding growth rate of 0.36 year^{-1} and a period of

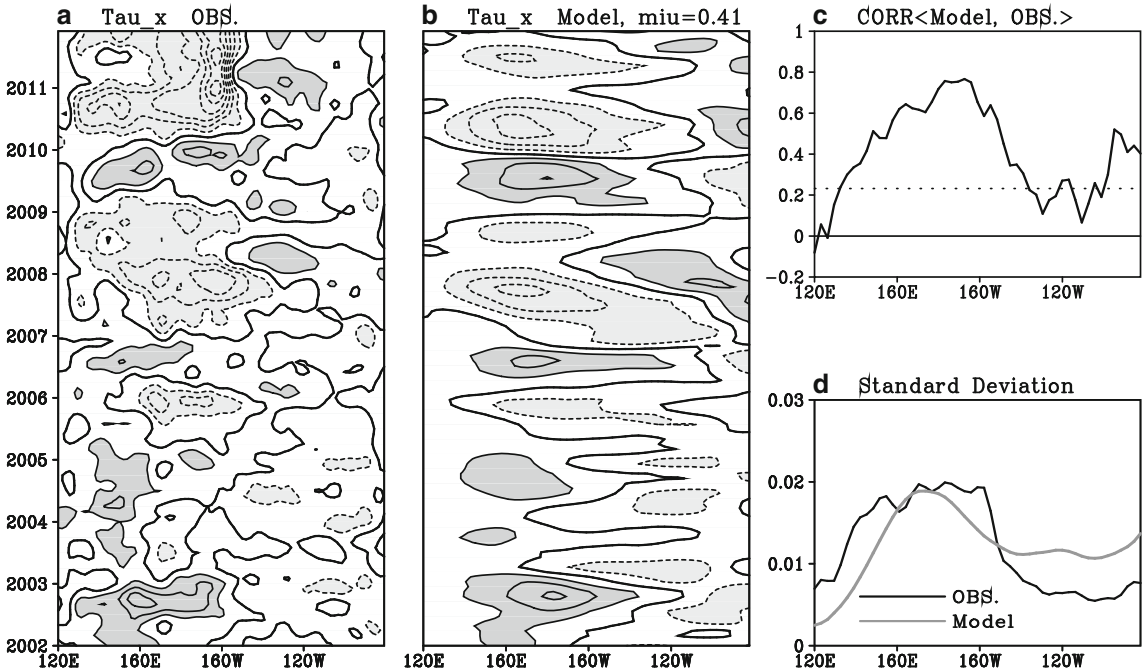

Fig. 6 Longitude–time cross-section of observed (**a**) and model simulated (**b**) equatorial wind stress anomalies for the period of 2002–2011. In the model, the air–sea coupling coefficient is set to 0.41. **c** The longitudinal distribution of correlation coefficient between observation and simulation. **d** The standard deviation of equatorial wind stress of observation (*black*) and simulation (*gray*) along the equator. The intervals for wind stress are 0.05 Pa

2.2 years. The evolving patterns of the eigenvectors of SST anomalies and SST tendency along with the heat budget terms of ZA and TH are shown in Fig. 7. The recharge model successfully captures the QB oscillation of ENSO with comparable observed amplitude in the central Pacific but without the westward propagation of SSTA (Fig. 7a). It is clear that the contribution of the ZA term is much greater than (equal to) the TH term in the central (eastern) Pacific (Fig. 7c, d). Moreover, the ZA term is in phase with the SST tendency, and it produces

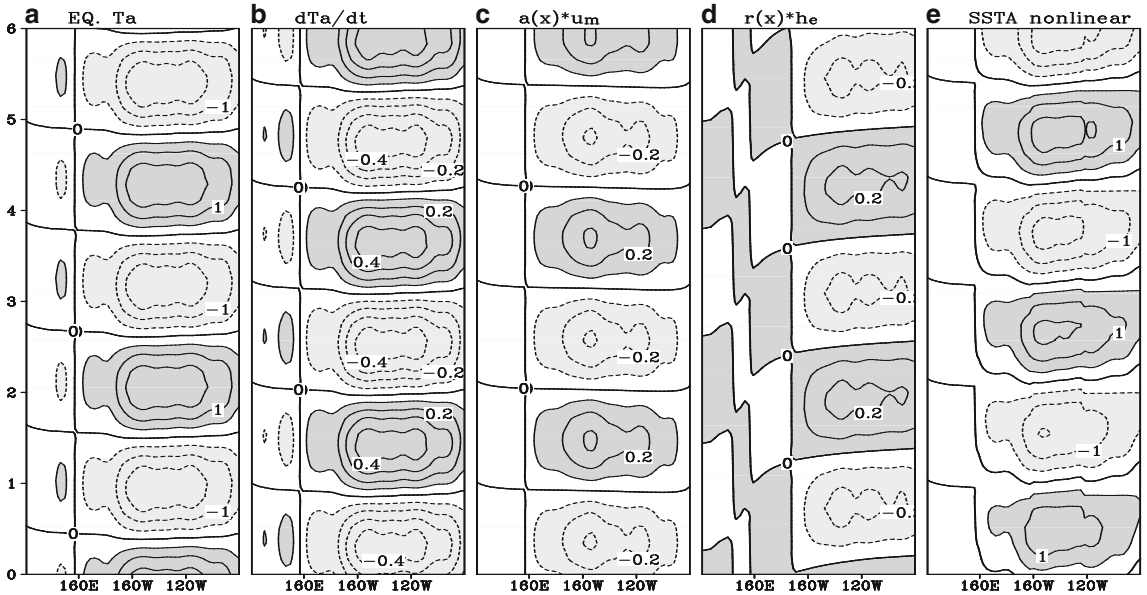

Fig. 7 Longitude–time cross-section of the eigenvectors of SST (**a**), SST tendency (**b**), zonal advective feedback (**c**) and thermocline feedback (**d**) anomalies along the equator. The eigenvectors and heat budget terms are derived from the stability analysis of the recharge model for the basic state of 2002–2012. The intervals for (**a**) are 0.5 °C, and for (**b**) to (**d**) are 0.1 °C/month, respectively. Evolution of equatorial SST anomalies in the nonlinear run is shown in **e**. The *y*-axis indicates year

the negative tendency even when the TH term is still positive, which in whole indicate that the ZA term contributes to both the growth and transition of ENSO. Meanwhile, the TH term contributes mainly in the eastern Pacific, and it serves as an accelerator after the ZA term causes the initial negative tendency. To summarize, the anomalous zonal sea currents reverse their signal at peak phase and start to weaken the peak property of the thermocline to drive ENSO towards the decaying stage. All these features revealed by the model are consistent with observations (Kug et al. 2009; Ren and Jin 2013), and also confirm the applicability of this model for the research of central Pacific ENSO.

In order to further connect the linear model result with the somewhat nonlinear observation, equatorial SST anomalies from a 10-year of nonlinear model run are shown in Fig. 7e. In the nonlinear model, the only change is that a term of $-3h_e^3$, the same form of simple thermocline nonlinearity (Jin 1997b), is added to the SST anomalies equation (Eq. 5). The model is then integrated for 10 years with initial SST anomalies of 0.1 °C along the equator. The evolution of equatorial SST anomalies shows a quasi-biennial ENSO-like oscillation, and has the variation center on the central and eastern Pacific. It is similar to the SST eigenvector from the linear model (Fig. 7a), and is also very close to the observation shown in Fig. 2a.

Another stability analysis is designed under the same manner but using the mean state of 1982–2001. In this experiment, the leading unstable ENSO-like mode has an *e*-folding growth rate of 0.32 year^{-1} and an oscillation period of 5.5 years, which is consistent with the eigen-mode of the same period revealed by Kang et al. (2004). The evolving patterns of the eigenvectors of SST anomalies and SST tendency and the heat budget terms of ZA and TH for this mode are shown in Fig. 8. The SST anomalies pattern has large variations in the eastern Pacific and extends into the central Pacific, which is very close to the EP ENSO in that period. TH contributes at least two times more than ZA in the developing and decaying phases of this mode (Fig. 8c, d). Similar to the former case, TH contributes more in the eastern Pacific, whereas ZA only has a much weaker contribution concentrated in the central Pacific. Interestingly, just like in the former experiment, ZA provides negative feedback to reverse the SST anomalies when TH is still positive, suggesting that ZA provides the initial force to start the phase transition. Such a role of ZA in the EP ENSO revealed by this model is consistent with results of previous studies. For instance, Zhang et al. (2007) finds that ZA acts as a transition trigger of ENSO. Ren and Jin (2013), in their very recent study, report that ZA contributes to the phase transitions of both types of ENSO.

The stability analysis of the recharge model has confirmed the applicability of this model in the study of both types of ENSO. Also, the different leading ENSO-like eigen-modes confirm the sensitiveness of ENSO dependence on the mean states. Moreover, the results suggest that the ZA term contributes more than the TH term to ENSO in the period of 2002–2012 when the tropical Pacific displays a La Niña-like climate shift, whereas in the period of 1982–2001 the opposite is true. It also suggests that the ZA term provides the initial transition force to both types of ENSO, while the TH term contributes and accelerates the developing and decaying of ENSO. Honestly, this model fails in produces the westward propagation of SSTA as revealed by observation. A possible reason is that this model does not contain the nonlinear effect of zonal advection of temperature anomalies by total sea currents $((\overline{u}+u^{a})(dT^{a})/dx)$. As argued by Santoso et al. (2013), the interplay between the ENSO-related current anomaly and the mean current determines the propagation of ENSO SSTA. In the CP El Niño, the zonal current anomalies were relatively weak and could not overcome the mean westward current, therefore the effect of the westward total current weakened the eastward propagation associated with thermocline feedback but reinforced the westward propagation related to zonal advective feedback.

5 Summary

The quasi-biennial ENSO in the central Pacific over the recent decade (2002–2012) are examined in this study. The results from observation and model reveal that the quasi-biennial ENSO largely depends on the zonal advective feedback, which is favored by the tropical Pacific mean state of that period. The stability analyses of a simple model also confirm the independence of central Pacific ENSO from the eastern Pacific ENSO under the current basic state of the tropical Pacific.

The observational evidence presented in this paper indicates that there are four ENSO warming events occurred in the central Pacific during 2002–2012, and three of them show a westward propagation of SST anomalies, particularly over the central and western Pacific during their decaying stages. The zonal advective feedback is responsible for the fast-paced central Pacific ENSO events, because the SST anomalies are tightly associated with the anomalous zonal sea currents related to oceanic waves. The zonal sea current anomalies lead the SST and thermocline depth anomalies by 1/4 cycle, so they are the key factors that cause the recharge of heat content before El Niño bursting and the discharge process when El Niño is at the mature phase. The variation of thermocline is consistent with the recharge/discharge theory (Jin 1996, 1997a, b).

Using a two-strip recharge model with the free parameters derived from the Pacific mean state in the recent decade, it is revealed that the quasi-biennial mode is the only unstable ENSO-like oscillatory mode. In the mode, the SST anomalies resemble the pattern of observed central Pacific ENSO, but without the westward propagation. Its SST tendency is dominated by the zonal advective feedback, which is also the key

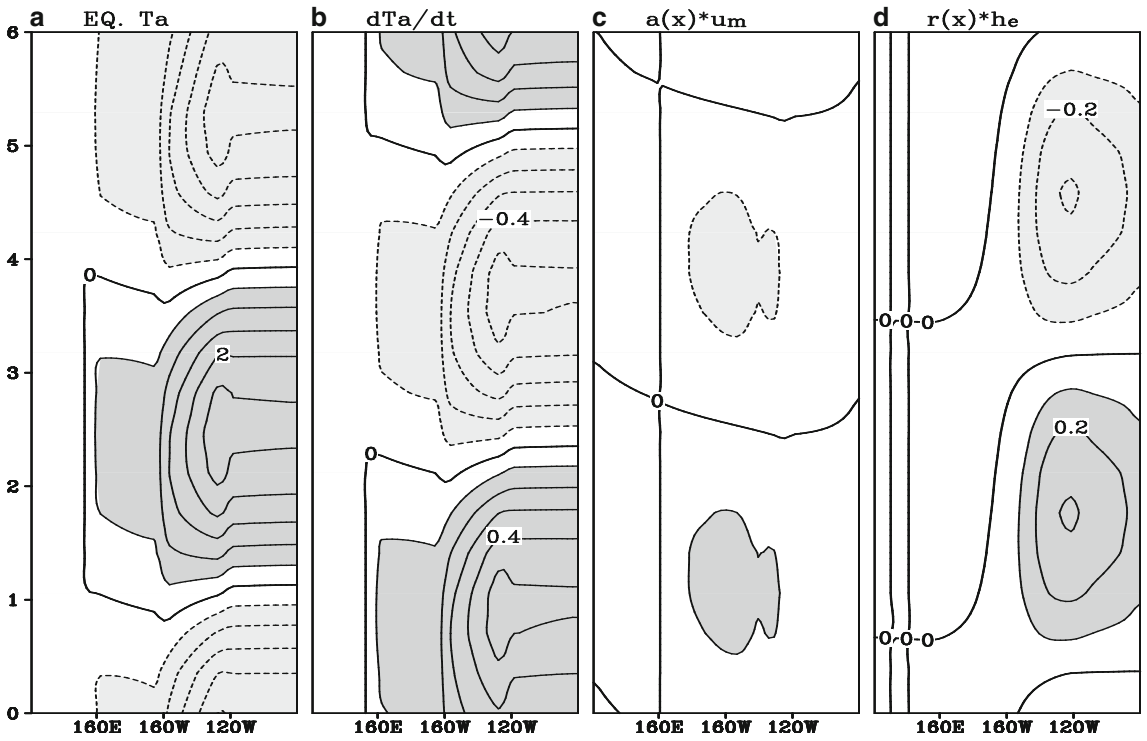

Fig. 8 Same as Fig. 7, except for the basic state of 1982–2001. The intervals for **a** are 0.5 °C, and for **b** to **d** are 0.1 °C/month, respectively. The *y*-axis indicates year

factor of the phase transition. Moreover, the ENSO-like mode is sensitive to the mean state. In a similar eigen-analysis using the mean state of 1982–2001, the leading ENSO-like mode is the quasi-quadrennial mode with SST variation centered in the eastern Pacific, and it is controlled by the slow variation of the thermocline. In other words, it resembles the eastern Pacific ENSO and dynamically it behaves like the recharge oscillator (Jin and Neelin 1993; Jin 1997b, 2001).

The eigen-analysis also indicates that the sensitiveness of the leading mode results from the shift of the tropical Pacific basic state around the beginning of this century. Compared to the early period of 1982–2001, the zonal temperature gradient of the Pacific strengthens while the response of the subsurface temperature to the vertical moment of thermocline weakens in the recent decade. Thus, the zonal advection of the mean temperature gradient by the anomalous sea current becomes more efficient in generating the SST anomalies in the central equatorial Pacific where the mean temperature gradient is largest. Considering the intrinsic high-frequency of the zonal advective feedback (FP01), the recent fast-paced ENSO activities in the central Pacific is suggested due to the dominance of zonal advective feedback favored by the basic state conditions in the recent decade.

However, the understanding on the relationship between mean states and ENSO's features is still controversial. For example, the theoretical works of FP01 and BJ08 supported that the mean state change can cause the shift of ENSO type, while some recent observational evidences favor a conclusion that the more frequent occurrence of CP El Niño events caused the mean climate change (Lee and McPhaden 2010; McPhaden et al. 2011). So far, the mean state and ENSO seem to be on a chain, as the chicken and egg problem, the present evidences are inadequate to distinguish the causal factor, which is also beyond the aims of this paper. This paper just attempts to provide a one-way approach to understand the influence of the mean state change on ENSO pattern shift.

Our study supplements the theoretical explanation of the ENSO mechanism for the apparently different ENSO phenomenon over the recent decade. The model used in this study is extremely simplified with only the major physical processes, hence the results revealed here are purified to some extent. In the diagnoses and prediction study, more physical processes are needed to maximize our understanding of ENSO. For instance, the mean meridional currents are crucial in determining the meridional width of ENSO (Zhang et al. 2009, 2013), and the nonlinear dynamic heating will lead to the asymmetry between El Niño and La Niña (An and Jin 2001). This study provides solid evidences to demonstrate the importance of physical feedbacks and mean states in determining ENSO behaviors, which can serve as a theoretical basis in prediction of ENSO phenomena.

Acknowledgments Dr. Ruihuang Xie and Prof. Fei Huang are jointly sponsored by the National Basic Research Program of China (973 Program: 2010CB951403 and 2012CB955604) and National Natural Science Foundation of China (No. 40975038, 40830106, 41230420). Prof. F.-F. Jin

is jointly supported by National Science Foundation (NSF) Grants ATM1034798 and DOE Grant DE-SC0005110. Dr. Jian Huang is supported by National Public Benefit Research Foundation (Meteorology) (GYHY200906008). Dr. Xie thanks the Chinese Scholarship Council for providing financial support during visiting Prof. F.-F. Jin. The authors thank two anonymous reviewers for their assistance in evaluating this paper.

References

An S-I, Jin F-F (2001) Collective role of zonal advective and thermocline feedbacks in ENSO mode. J Clim 14:3421–3432

An S-I, Wang B (2000) Interdecadal change of the structure of the ENSO mode and its impact on the ENSO frequency. J Clim 13:2044–2055

An S-I, Jin F-F, Kang I-K (1999) The role of zonal advection feedback in phase transition and growth of ENSO on the Cane-Zebiak Model. J Meteorol Soc Jpn 77:1151–1160

Ashok K, Behera SK, Rao SA, Weng H, Yamagata T (2007) El Niño Modoki and its possible teleconnection. J Geophys Res 112, C11007

Barnett TP (1991) The interaction of multiple time scales in the tropical climate system. J Clim 4:269–285

Battisti DS, Hirst AC (1989) Interannual variability in a tropical atmosphere–ocean model: influence of the basic state, ocean geometry, and nonlinearity. J Atmos Sci 46:1687–1712

Behringer DW, Ji M, Leetmaa A (1998) An improved coupled model for ENSO prediction and implication for ocean initialization. Part I: the ocean data assimilation system. Mon Weather Rev 126:1013–1021

Bejarano L, Jin F-F (2008) Coexistence of equatorial coupled modes of ENSO. J Clim 21:3051–3067

Bonjean F, Lagerloef GSE (2002) Diagnostic model and analysis of the surface currents in the tropical Pacific Ocean. J Phys Oceanogr 32(10):2938–2954

Burgers G, Jin F-F, Oldenborgh GJ (2005) The simplest ENSO recharge oscillator. Geophys Res Lett 32, L13706

Cane MA, Sarachik ES (1981) The periodic response of a linear baroclinic equatorial ocean. J Mar Res 39:651–693

Cane MA, Munnich M, Zebiak SE (1990) A study of self-excited oscillations of the tropical ocean–atmosphere system. Part I: linear analysis. J Atmos Sci 47:1562–1577

Fedorov AV, Philander SG (2000) Is El Niño changing? Science 288: 1997–2002

Fedorov AV, Philander SG (2001) A stability analysis of tropical ocean–atmosphere interactions: bridging measurements and theory for El Niño. J Clim 14:3086–3101

Hu Z-Z, Kumar A, Jha B, Wang W, Huang B, Huang B (2012) An analysis of warm pool and cold tongue El Niños: air-sea coupling processes, global influences, and recent trends. Clim Dyn 38:2017–2035

Hu Z-Z, Kumar A, Ren H-L, Wang H, L'Heureux M, Jin F-F (2013) Weakened interannual variability in the tropical Pacific ocean since 2000. J Clim 26:2601–2613

Ji M, Leetmaa A, Derber J (1995) An ocean analysis system for seasonal to interannual climate studies. Mon Weather Rev 123:460–481

Jin F-F (1996) Tropical ocean–atmosphere interaction, the Pacific cold tongue, and the El Niño-Southern Oscillation. Science 274:76–78

Jin F-F (1997a) An equatorial ocean recharge paradigm for ENSO. Part I: conceptual model. J Atmos Sci 54:811–829

Jin F-F (1997b) An equatorial ocean recharge paradigm for ENSO. Part II: a stripped-down coupled model. J Atmos Sci 54:830–847

Jin F-F (2001) Low-frequency modes of the tropical ocean dynamics. J Clim 14:3874–3881

Jin F-F, An S-I (1999) Thermocline and zonal advective feedbacks within the equatorial ocean recharge oscillator model for ENSO. Geophys Res Lett 26:2989–2992

Jin F-F, Neelin JD (1993) Modes of interannual tropical ocean–atmosphere interaction—a unified view. Part I: numerical results. J Atmos Sci 50: 3477–3503

Jin F-F, Kug J, An S-I (2003) A near-annual coupled mode in the equatorial Pacific Ocean. Geophys Res Lett 30:1080

Jin F-F, Kim S-T, Bejarano L (2006) A coupled-stability index for ENSO. Geophys Res Lett 33, L23708

Kang I-S, An S-I, Jin F-F (2001) A systematic approximation of the SST anomaly equation for ENSO. J Meteorol Soc Jpn 79:1–10

Kang I-S, Kug J-S, An S-I, Jin F-F (2004) A near annual Pacific Basin mode. J Clim 17(12):2478–2488

Kao H-Y, Yu J-Y (2009) Contrasting eastern-Pacific and central-Pacific types of ENSO. J Clim 22:615–632

Kirtman BP (1997) Oceanic Rossby wave dynamics and the ENSO period in a coupled model. J Clim 10:1690–1704

Kug J-S, Jin F-F, An S-I (2009) Two-types of El Niño events: cold tongue El Nino and warm pool El Nino. J Clim 22:1499–1515

Kumar A, Hu Z-Z (2013) Interannual and interdecadal variability of ocean temperature along the equatorial Pacific in conjunction with ENSO. Clim Dyn. doi:10.1007/s00382-013-1721-0

Larkin NK, Harrison DE (2005) On the definition of El Niño and associated seasonal average U.S. weather anomalies. Geophys Res Lett 32:L13705

Lee T, McPhaden MJ (2010) Increasing intensity of El Niño in the central equatorial Pacific. Geophys Res Lett 37, L14603

McPhaden MJ (2012) A 21st century shift in the relationship between ENSO SST and warm water volume anomalies. Geophys Res Lett 39, L09706

McPhaden MJ, Lee T, McClurg D (2011) El Niño and its relationship to changing background conditions in the tropical Pacific Ocean. Geophys Res Lett 38, L15709

Meinen CS, McPhaden MJ (2000) Observations of warm water volume changes in the equatorial Pacific and their relationship to El Niño and La Niña. J Clim 13:3551–3559

Neelin JD, Jin F-F (1993) Modes of interannual tropical ocean–atmosphere inter-action—a unified view Part II: analytical results in weakly-coupled cases. J Atmos Sci 50:3504–3522

Picaut J, Masia F, du Penhoat Y (1997) An advective–reflective conceptual model for the oscillatory mature of the ENSO. Science 277: 663–666

Rasmusson EM, Carpenter TH (1982) Variations in tropical sea surface temperature and surface wind field associated with the Southern Oscillation/El Niño. Mon Weather Rev 110:354–384

Rayner NA, Parker DE, Horton EB, Folland CK, Alexander LV, Rowell DP, Kent EC, Kaplan A (2003) Global analyses of sea surface temperature, sea ice, and night marine air temperature since the late nineteenth century. J Geophys Res 108(D14):4407

Ren H-L, Jin F-F (2011) Niño indices for two types of ENSO. Geophys Res Lett 38, L04704

Ren H-L, Jin F-F (2013) Recharge oscillator mechanisms in two types of ENSO. J Clim 26(17):6506–6523

Ren H-L, Jin F-F, Stuecker MF, Xie R-H (2013) ENSO regime change since the late 1970s as manifested by two types of ENSO. J Meteorol Soc Jpn 91(6):835–842

Santoso A, McGregor S, Jin F-F, Cai W, England MH, An S-I, McPhaden MJ, Guilyardi E (2013) Late-twentieth-century emergence of the El Nino propagation asymmetry and future projections. Nature 504: 126–130

Schopf PS, Suarez MJ (1988) Vacillations in a coupled ocean–atmosphere model. J Atmos Sci 45:549–566

Thual S, Dewitte B, An S-I, Ayoub N (2011) Sensitivity of ENSO to stratification in the recharge–discharge conceptual model. J Clim 2011(24):4332–4349

Trenberth KE (1976) Spatial and temporal variations of the Southern Oscillation. Q J R Meteorol Soc 102:639–654

Trenberth KE (1984) Signal versus noise in the Southern Oscillation. Mon Weather Rev 112:326–332

Vimont DJ, Battisti DS, Hirst AC (2001) Footprinting: a seasonal connection between the tropics and mid-latitudes. Geophys Res Lett 28(20):3923–3926

Vimont DJ, Wallace JM, Battisti DS (2003) The seasonal footprinting mechanism in the Pacific: implications for ENSO. J Clim 16:2668–2675

Vimont DJ, Alexander M, Fontaine A (2009) Midlatitude excitation of tropical variability in the Pacific: the role of thermodynamic coupling and seasonality. J Clim 22(3):518–534

Wang B, An S-I (2005) A method for detecting season-dependent modes of climate variability: S-EOF analysis. Geophys Res Lett 32, L15710

Weng H, Ashok K, Behera SK, Rao SA, Yamagata T (2007) Impacts of recent El Niño Modoki on dry/wet conditions in the Pacific rim during boreal summer. Clim Dyn 29:113–129

Xiang B-Q, Wang B, Li T (2013) A new paradigm for the predominance of standing Central Pacific Warming after the late 1990s. Clim Dyn 41(2):327–340

Xie R-H, Huang F, Ren H-L (2013) Subtropical air–sea interaction and the development of the Central Pacific El Niño. J Ocean Univ China 12(2):260–271

Yeh S-W, Kug J-S, Dewitte B, Kwon MH, Kirtman BP, Jin F-F (2009) El Niño in a changing climate. Nature 461:511–515

Yu J-Y, Kim S-T (2011) Relationships between extratropical sea level pressure variations and the Central Pacific and Eastern Pacific types of ENSO. J Clim 24:708–720

Zebiak SE (1986) Atmospheric convergence feedback in a simple model for El Niño. Mon Weather Rev 114:1263–1271

Zebiak SE, Cane MA (1987) A model El Niño and Southern Oscillation. Mon Weather Rev 115:2262–2278

Zhang Q, Kumar A, Xue Y, Wang W, Jin F-F (2007) Analysis of the ENSO cycle in the NCEP coupled forecast model. J Clim 20:1265–1284

Zhang W-J, Li J-P, Jin F-F (2009) Spatial and temporal features of ENSO meridional scales. Geophys Res Lett 36, L15605

Zhang W, Jin F-F, Li J-P, Ren H-L (2011) Contrasting impacts of two-type El Niño over the western north Pacific during boreal autumn. J Meteorol Soc Jpn 89:563–569

Zhang W, Jin F-F, Zhao J-X, Li J-P (2013) On the bias in simulated ENSO SSTA meridional widths of CMIP3 models. J Clim 26:3173–3186